


Article

Adaptive Controller of the Major Functions for Controlling a Drive System with Elastic Couplings

Dung Tran Anh ¹ and Thang Nguyen Trong ^{2,*} 

¹ Faculty of Electrical-Electronic Engineering, Vietnam Maritime University, Haiphong 181810, Vietnam; trananhdung70@gmail.com

² Department of Electrical Engineering and Automation, Haiphong Private University, Haiphong 181810, Vietnam

* Correspondence: phdthangnguyen@yahoo.com; Tel.: +84-168-846-8555

Received: 23 January 2018; Accepted: 27 February 2018; Published: 1 March 2018

Abstract: In any drive system, there are always couplings between the motor and the load. Since the hardness of these couplings is finite, they have elastic properties, causing unwanted vibration and negatively affecting system quality. When the couplings are springs with nonlinear characteristics, control is particularly difficult because it is very difficult or impossible to define the parameters of the controlled object. To solve these difficulties, this article proposes an adaptive controller of the major functions for controlling a drive system with nonlinear elastic couplings of unidentified parameters. For the proposed control system, we measure the response speed of the object, use a Luenberger observer to estimate the state variables of the system, and use an adaptive controller to control the system. The experimental results demonstrate that the control object can be controlled without knowing the parameters: the control quality of the system is very good, close to that of a system with a hard coupling, there is no vibration or overshoot, and the transition time is small.

Keywords: adaptive; controller; major function; elastic coupling

1. Introduction

Speed and position control systems are widely used in industry when loads connect to a motor drive by couplings of finite stiffness. This finite stiffness causes oscillations and has negative effects on the quality of both electrical and mechanical systems. Studies have shown the negative effects of elastic couplings in several applications, such as rolling mills [1,2], electric vehicles [3], wind generators [4,5], controlling robots [6], and paper production [7].

Proportional-integral (PI) controllers are the most commonly used for controlling the speed and position of elastic coupling systems, for example, in industry [8], or in the speed and location control systems of vehicles [9]. Some studies have improved the control quality of elastic coupling systems and reduced their vibration by adjusting the PI controller parameters [10]. However, PI controllers do not provide feedback of the system states, and the pole placement of these system provides minimal oscillation reduction [11]. PID controllers could increase oscillation reduction, but they are highly sensitive to external noise.

State space control offers a promising direction for improving the quality of elastic coupling systems [12]. How state space control works has been described elsewhere [13]. The advantage of state space control is that it allows for free pole placement in the closed system, but it is difficult to build the controller, and all state variables must be measured or estimated. Additionally, a linear controller is not suitable for nonlinear elastic coupling systems, so that its effectiveness and quality are low.

Nonlinear controllers have been proposed to control drive systems with elastic couplings, such as a sliding mode control [14–17], neural control or fuzzy sliding mode control [18,19], flatness based

control [20,21], a control method based on identification allowing for robust $H\infty$ [22], and a predictive controller with a state space model [23]. However, for a high-quality control system, these methods require knowing exactly the parameter values of the control object. But in drive control systems with elastic couplings, the parameters of the control object are difficult or impossible to determine. Therefore, we set out to improve the quality of a nonlinear drive system with elastic couplings and unknown object parameter values. This research is the first one using an adaptive controller of the major functions for controlling a drive system with elastic couplings. As will be seen, the quality of the whole system is very high, there is no vibration, and the transition time is short.

What follows in this paper describes the characteristics and dynamic equations of a drive system with elastic couplings (Section 2), our proposed adaptive controller of the major functions (Section 3), and the algorithm installation process and experimental results (Section 4). In Section 5, our conclusions are presented.

2. The Nonlinear Model of the Drive System with Elastic Couplings

Consider an elastic object which includes n blocks linked together by elastic couplings with slits. Such a system is shown in Figure 1.

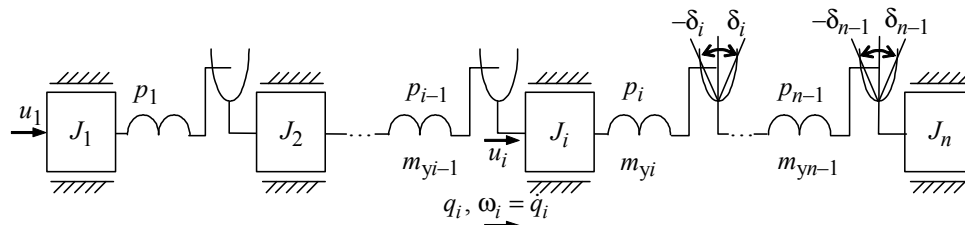


Figure 1. Drive system with elastic couplings and slits.

The differential equations of the control object are as follows:

$$\begin{cases} \dot{\omega}_i = \frac{1}{J_i} [f_{y,i-1} - f_{yi} + b_i u_i(t)], & i = \overline{1, n}; \\ \dot{m}_{yi} = p_i (\omega_i - \omega_{i+1}), & i = \overline{1, n-1}; \end{cases} \quad (1)$$

where

- $\omega_i, i = \overline{1, n}$ are the speeds or angular velocities of the blocks;
- $J_i, i = \overline{1, n}$ are the inertias of the blocks; and
- $f_{yi}, i = \overline{1, n-1}$ are the elastic forces when taking account of the slit ($2\delta_i$) between joints, f_{yi} calculated as follows:

$$f_{yi} = \begin{cases} m_{yi} - p_i \delta_i, & \text{if } m_{yi} \geq p_i \delta_i; \\ 0, & \text{if } |m_{yi}| < p_i \delta_i; \\ m_{yi} + p_i \delta_i, & \text{if } m_{yi} \leq -p_i \delta_i; \end{cases} \quad (2)$$

Additionally:

- $u_i, i = \overline{1, n}$ are the control signals which impact on the blocks with the coefficient b_i , and
- $m_{yi}, i = \overline{1, n-1}$ are the elastic moments, which are calculated as follows:

$$m_{yi} = p_i (q_i - q_{i+1}), \quad i = \overline{1, n-1}; \quad (m_{y0} = m_{yn} = 0) \quad (3)$$

In Equation (3), $q_i, i = \overline{1, n}$ are the block movements or the block rotation angles, and $p_i, i = \overline{1, n-1}$ are the elastic coefficients of the couplings. Since ω_i, m_{yi} are chosen as status variables, the control object has $(2n - 1)$ orders.

Typically, the parameter values of an elastic control object cannot be directly measured by sensors. We can only measure the speeds of the control object. However, our control object is fully controllable and observable. It is therefore possible to apply state observation for controlling a drive system with nonlinear elastic couplings when parameters are unspecified. Several methods can be used to estimate the system states; for example, Luenberger observation, extended Luenberger observation, Kalman filter, or disturbance observation [24–26].

In this paper, we experiment on the physical system of a DC motor drive system. The system consists of two blocks that link together via a nonlinear elastic coupling. The system is shown in Figure 2.

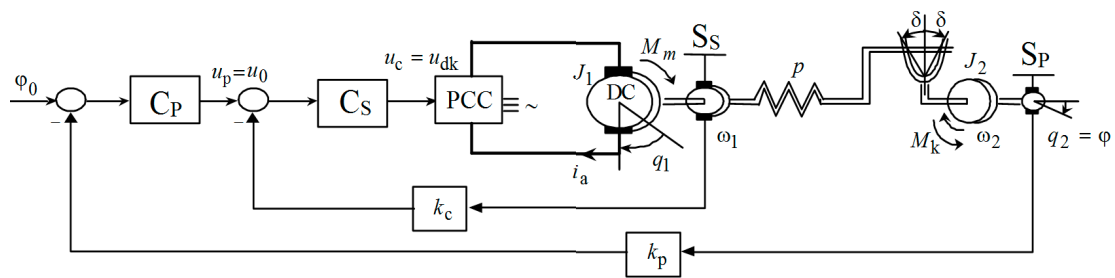


Figure 2. Physical model of the drive system with a nonlinear elastic coupling.

Our goal is to accurately control the position of the second disk block. Our proposed control system has two closed loops: an inner control loop, to control the speed of the load, and an outer control loop, to control the position of the load. In Figure 2, DC denotes the direct current motor; PCC denotes the power control circuit; C_P denotes the position controller; C_S denotes the speed controller; S_S denotes the speed sensor; and S_P denotes the position sensor. There is not a current loop in this experimental system, firstly, because the control object is a drive system with elastic couplings; adding a current loop would make it more complex and the mission of building adaptive controller more difficult. Secondly, the main missions of our control system are controlling position and damping elastic oscillations, rather than controlling the current. Finally, since the DC motor in the system has a large reserve, it can accommodate up to 10 times the normal current.

Our goals are ensuring that real position of the second disk block is close to the desired position and minimizing elastic oscillations in the system. The authors propose adaptive controllers to solve the above mission. Controller parameters are optimized to increase the rapidity of the transition processes. The control signal impacts the inner loop (the speed control loop) in order to decrease the order of the adaptive control system. Assuming a small electromagnetic time constant, the equations of the drive system are:

$$\begin{cases} \dot{\omega}_2 = \frac{1}{J_2} f_y - \frac{1}{J_2} M_k \\ \dot{m}_y = -p\omega_2 + p\omega_1 \\ \dot{\omega}_1 = -\frac{1}{J_1} f_y - \frac{k_m i (k_e i + k_c i k_y \beta_c)}{J_1 R_a} \omega_1 + \frac{k_m i k_y \beta_c}{J_1 R_a} u \end{cases} \quad (4)$$

where

- ω_1, ω_2 are the rotation speeds of the first disk block and the second disk block and m_y is the elastic moment when ignoring the slit;
- J_1, J_2 are the inertia moments of the first disk block and the second disk block; and
- f_y is the elastic force when taking account of the slit (2δ) in the elastic coupling:

$$f_y = \begin{cases} m_y - p\delta, & \text{if } m_y \geq p\delta, \\ 0, & \text{if } |m_y| < p\delta, \\ m_y + p\delta, & \text{if } m_y \leq -p\delta; \end{cases} \quad (5)$$

- M_k is the friction moment, and is calculated as follows:

$$M_k = M_{k0} \text{sign} \omega_2, M_{k0} = (0.1 \div 0.3) M_n \quad (6)$$

where M_n is the norm moment of the motor. Additionally:

- p is the elastic coefficient of the coupling,
- k_e and k_m are the coefficients of the motor structure, k_y is the transmission coefficient of the converter, k_c is the transmission coefficient of the speed sensor, β_c is the proportional coefficient of the speed controller, and R_a is the armature resistance of the DC motor. i denotes the gear transmission coefficient between the first disk block and the drive motor.
- u is the overall control signal: $u = u_0 + u_a$, with $u_0 = u_p$ the desired speed signal and u_a is the control signal which needs to be determined.

The outer loop control is the position control which is presented by the following equation:

$$\dot{\varphi} = \omega_2; u_p = (\varphi_0 - k_p \varphi) \beta_p \quad (7)$$

where φ is the position or the rotation angle of the load, k_p is the transmission coefficient of the position sensor, β_p is the proportional coefficient of the position controller, and φ_0 is the desired position.

Usually it is difficult to determine the moment of inertia and elastic coefficients, so we approximate those values: $J_1 = J_{01}$, $J_2 = J_{02}$, and $p = p_0$. Named: $a_1 = 1/J_{02}$; $a_2 = p_0$; $a_3 = -1/J_{01}$; $a_4 = -k_m i (k_e i + k_c i k_y \beta_c) / (J_{01} R_a)$; $b = k_m i k_y \beta_c / (J_{01} R_a)$. Equation (2) can be rewritten in matrix form and linearly as:

$$\dot{\underline{x}} = \mathbf{A} \underline{x} + \mathbf{B} u; \quad (8)$$

where

$$\mathbf{A} = \begin{bmatrix} 0 & a_1 & 0 \\ -a_2 & 0 & a_2 \\ 0 & a_3 & a_4 \end{bmatrix}; \mathbf{B} = \begin{bmatrix} 0 \\ 0 \\ b \end{bmatrix}; \underline{x} = \begin{bmatrix} \omega_2 \\ m_y \\ \omega_1 \end{bmatrix} \quad (9)$$

3. Control System Based on an Adaptive Controller of the Major Functions

In this section, we propose an adaptive controller to extinguish elastic oscillations and decrease the transaction time in cases where some parameters are undefined. The proposed method uses an adaptive controller of the major functions to minimize the effect of nonlinear elements such as slits and friction.

Consider a nonlinear control object which is described by the following differential equations:

$$\dot{\underline{x}}(t) = \underline{f}(\underline{x}, \underline{u}, t) \quad (10)$$

where $\underline{x} = (x_1, x_2, \dots, x_n)^T$ is the state vector of the control object, $\underline{x} \in R^n$. R^n is the Euclidean space that includes n dimensions, $\underline{u} = (u_1, u_2, \dots, u_m)^T$ is the control vector, $m < n$ and $\underline{f}(\cdot) = (f_1(\cdot), f_2(\cdot), \dots, f_n(\cdot))^T$ is the function vector that includes n dimensions. It is continuous according to $\underline{x}, \underline{u}$ and continuous in parts according to time (t) in the domain:

$$\Gamma_t = \{\underline{x}, \underline{u}, t : \|\underline{x}\| < \eta; \eta = \text{const}(\eta > 0); \underline{u} \in U; t \geq t_0, t_0 \in R\} \quad (11)$$

U denotes the set of the ability control signals, $\|\cdot\|$ denotes the norm of the vector, and T denotes the transposition of the matrix.

Assuming that the original object is represented by the equation:

$$\dot{\underline{x}} = \mathbf{A}(\underline{x}, t)\underline{x} + \mathbf{B}(\underline{x}, t)\underline{u}(t) \tag{12}$$

where $\mathbf{A}(\underline{x}, t)$, $\mathbf{B}(\underline{x}, t)$ are matrixes of a suitable size. The matrix $\mathbf{B}(\underline{x}, t)$ is limited. The matrix $\mathbf{A}(\underline{x}, t)$ can be written in the double sum form:

$$\mathbf{A}(\underline{x}, t) = \left\{ \sum_{q=0}^p \left[\sum_{r=1}^n \mathbf{A}_{qr}(\underline{x}, t) f_{qr}^\theta(x_r) \right] \right\} \tag{13}$$

$\mathbf{A}_{qr}(\underline{x}, t)$ are limited matrixes, but $f_{qr}^\theta(x_r)$ are scalar functions which may not be limited, and $f_{qr}^\theta(x_r)$ depends only on the r th element of the state vector. When $\|x\| \rightarrow +\infty$, the index q in Equation (13) is used to distinguish the functions $f_{qr}^\theta(x_r)$ with the different increase speeds. The function with the larger index q will increase faster, which means that:

$$\lim_{|x_r| \rightarrow +\infty} \frac{|f_{q+1,r}^\theta(x_r)|}{|f_{qr}^\theta(x_r)|} = +\infty \tag{14}$$

where $p = \max p_r$ and p_r is the number of increase functions with the element (x_r) . The increase speed of the functions can be compared to the exponential function x_r^h . The smallest coefficient is h in order that $\lim_{|x_r| \rightarrow +\infty} |f_{qr}^\theta(x_r)/x_r^h| < \infty$ is the increment of the scalar function $f_{qr}^\theta(x_r)$.

Assuming that the mission is to build adaptive control law $\underline{u}(t)$ so that that the trajectory of the control object follows the trajectory of the reference model, as:

$$\dot{\underline{x}}_M(t) = \mathbf{A}_M \underline{x}_M(t) + \mathbf{B}_M \underline{u}_0(t) \tag{15}$$

where $\mathbf{A}_M, \mathbf{B}_M$ are the constant matrixes and $\underline{u}_0(t)$ is the vector of the desired value. The target of the control system is expressed by the following equation:

$$\lim_{t \rightarrow \infty} \|\underline{x}(t) - \underline{x}_M(t)\| = \lim_{t \rightarrow \infty} \|\underline{e}(t)\| < D \tag{16}$$

where D is any coefficient which is greater than zero and $\underline{e}(t)$ is the vector of the control error.

The control signal is the sum of the two components:

$$\underline{u}(t) = \underline{u}_a(t) + \underline{u}_0(t) \tag{17}$$

where $\underline{u}_a(t)$ is the adaptive component, which is represented in the following equation:

$$\underline{u}_a(t) = \left\{ \sum_{q=0}^p \left[\sum_{r=1}^n \mathbf{K}_{qr}^A(t) f_{qr}(x_r) \right] \right\} \underline{x} + \mathbf{K}_B(t) \underline{u}_0(t) \tag{18}$$

$\mathbf{K}_{qr}^A(t), \mathbf{K}_B(t)$ are the matrixes with the adjustable coefficients, and are determined by the following equations:

$$\begin{cases} \dot{\mathbf{K}}_{qr}^A(t) = -f_{qr}(x_r) \mathbf{\Gamma}_{qr}^A \mathbf{B}_M^T \mathbf{P} \underline{e} x^T - \mathbf{\Lambda}_{qr}^A \mathbf{K}_{qr}^A(t) \\ \dot{\mathbf{K}}_B(t) = -\mathbf{\Gamma}_B \mathbf{B}_M^T \mathbf{P} \underline{e} u_0^T - \mathbf{\Lambda}_B \mathbf{K}_B(t) \end{cases} \tag{19}$$

$\mathbf{\Gamma}_{qr}^A, \mathbf{\Lambda}_{qr}^A, \mathbf{\Gamma}_B, \mathbf{\Lambda}_B$ are the positive symmetric matrixes, \mathbf{P} is the positive symmetric matrix which is the solution of the Lyapunov equation:

$$\mathbf{A}_M^T \mathbf{P} + \mathbf{P} \mathbf{A}_M = -\mathbf{G} \tag{20}$$

\mathbf{G} is the positive symmetric matrix which has been known.

The functions in Equations (18) and (19) are chosen in order to satisfy the relationship:

$$\left| \frac{f_{qr}^\theta(x_r)}{f_{qr}(x_r)} \right| \leq a_{qr} \text{ if } |x_r| \leq b_{qr}$$

where a_{qr}, b_{qr} are the positive coefficients. $f_{qr}(x_r)$ are the major functions, and $f_{qr}^\theta(x_r)$ are the increase functions. The control law, Equation (18), combined with the tuning algorithm, Equation (19), is named the adaptive controller of the major functions.

4. Setting up the Algorithm and Running the Experimental System

The authors built an experimental system of a drive with elastic coupling based on the structure of the control object presented in Section 2 and the adaptive algorithm presented in Section 3. This system consists of two blocks which are connected together by elastic coupling. The experimental system is shown as Figure 3.

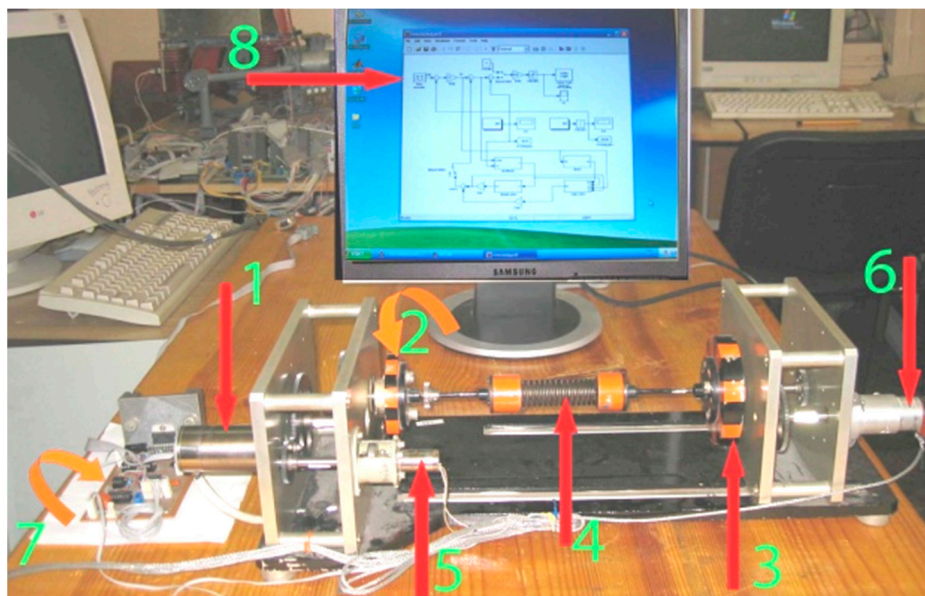


Figure 3. The experimental system of the drive with the elastic coupling.

The experimental system consists of a (1) DC Motor; (2) first spin disc block; (3) second spin disc block; (4) elastic coupling (the spring); (5) speed sensor; (6) position sensor; (7) power control circuit; and (8) computer screen.

The elastic coupling (spring) is the cause of the elastic oscillations and negative effects on system quality. Difficulties in controlling the system result from several parameters of the control object not being correctly defined, for example, the inertia moment and the elasticity coefficient, and from the control object's nonlinear elements, such as the slit and friction. To extinguish the elastic oscillations, the authors set up an adaptive control system for the major functions in order to control the position of the second block. The experimental system is designed according to the scheme shown in Figure 4.

The power control circuit receives the control signal from the computer through the Advantech PCI-1711 card, then controls the DC motor that drives the movement of the disk blocks. The power control circuit is a nonlinear system; its input is the control voltage and its output is the voltage supplied to the armature of the DC motor. The nonlinearity of the power control circuit is much less significant than that of the slit and friction. The equation for the experimental power control circuit model uses the coefficient (k_y). Since the proposed adaptive controller can control a nonlinear object of unidentified parameters, it is not necessary to consider the nonlinear parameters of the power control circuit.

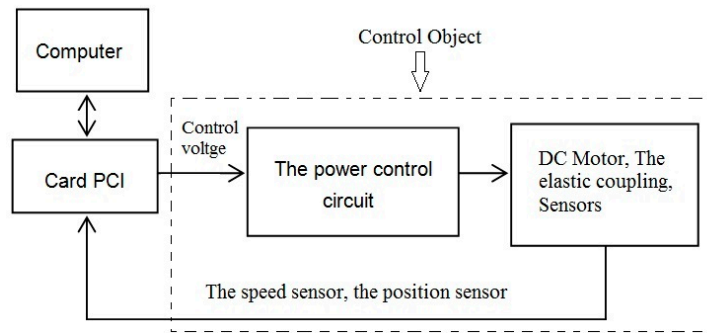


Figure 4. The connection diagram of the system.

The speed sensor is used for measuring the feedback-speed value of the first disk block. The position sensor is used for measuring the feedback-position value of the second disk block. The values from the sensors are sent to the computer through the PCI-1711 card.

In short, the control object is a collection of elements as follows: power control circuit, DC motor, elastic coupling, and sensors. The input of the control object is the control voltage of the power control circuit, the output of the control object is the signal of the position sensor of the second disk block. The input and output of the control object are connected to the controller (computer) through the PCI card. Thus, the control object is a complex nonlinear object and it is difficult to determine exactly the parameters.

The experimental system’s purpose is to control the second disk block’s position, extinguishing elastic oscillations and increasing the rapidity of the drive system. The problem of position control is solved by the position loop; that is, the outer loop. The challenge of extinguishing oscillation and increasing rapidity is solved by the adaptive controller, which impacts the inner loop.

Our real-time controller was built using Matlab Simulink software (version 8.4), as shown in Figure 5.

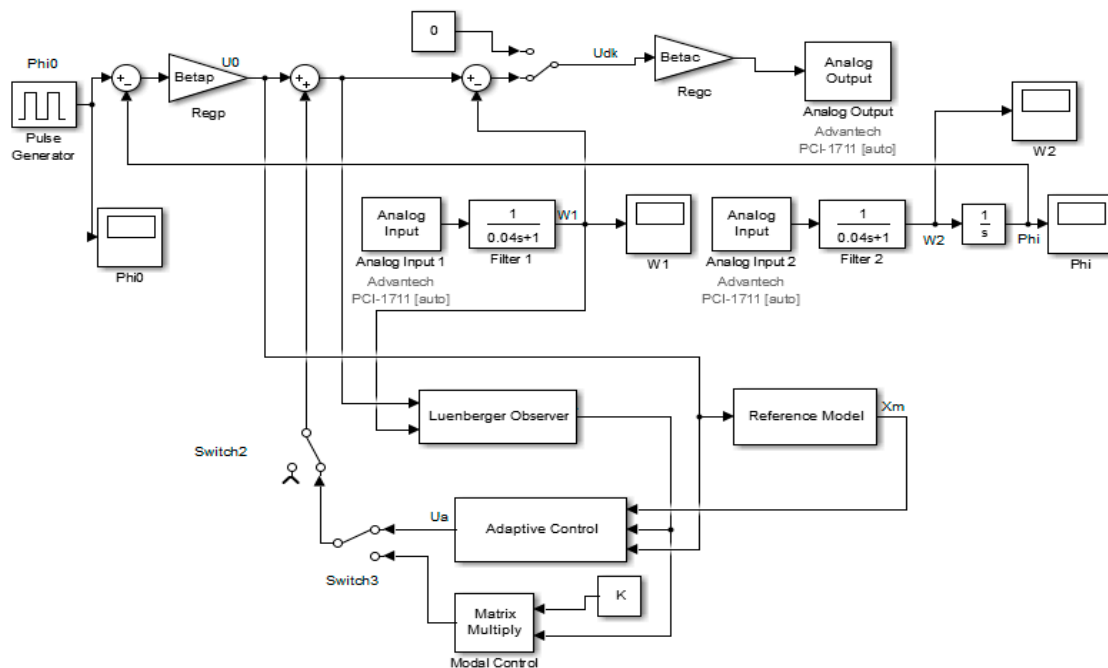


Figure 5. The structure of the real-time controller.

The control structure consists of the main following blocks:

- (1) The reference model is built in accordance with Equation (15). To extinguish the elastic oscillations, the matrixes \mathbf{A}_M , \mathbf{B}_M are built by the modal method, which is a pole placement control method [27,28].
- (2) For the Luenberger observer, the computer processes the sensor signals according to the Luenberger algorithm [29,30] in order to recreate the state vector of the control object. This state vector consists of three components: ω_2, m_y, ω_1 .
- (3) The adaptive control block is built based on parameter adjustment principles of the adaptive major functions controller (according to Equations (18) and (19)) so that the dynamic characteristic of the control object is close to that of the reference model and the effects of the nonlinear elements are minimal. In the adaptive algorithms shown in Equations (18) and (19), the state vector of the control object is replaced by the state vector of the Luenberger observer.

Experimentally, we used a non-adaptive modal control module for comparison with our adaptive controller.

The algorithms generate the control signals, which control the DC motor.

It was very difficult or impossible to determine the parameters of the experimental system. However, based on the parameter values of the devices in the system provided by the manufacturers, the parameter values of the experimental system were estimated as described below:

- (1) The parameters of the DC motor: norm power $P_n = 9.25$ W; norm speed $n_n = 4500$ rpm; norm moment $M_n = 0.0196$ Nm; norm voltage $U_n = 27$ V; norm current $I_n = 0.7$ A; efficiency $\eta = 49\%$; armature resistor $R_a = 11 \Omega$, coefficient $k_e = 0.041$; and coefficient $k_m = 0.028$.
- (2) The other parameters: $k_y = 2.78$; $k_c = 0.0098$ V·s/rad; $\beta_c = 8.047$; $k_p = 0.0412$ V/rad; $\beta_p = 149.12$; $J_{01} = 0.004$ kg·m²; $J_{02} = 0.003$ kg·m²; and $p_0 = 1.5$ Nm/rad.

We set the adaptive algorithm with the major functions based on Equations (18) and (19) using a simplified approach of ignoring all major functions and considering only the largest order function $f_{pr}(w_r)$, which is the exponential equation of each state variable x_r . For example, the slit function refers to the elastic moments (m_y) and the friction function refers to the speed of the second disk block (ω_2). Therefore, the major functions are described as follows:

$$f_{p2}(m_y) = \hat{m}_y^{p2}; f_{p1}(\omega_2) = \hat{\omega}_2^{p1}; f_{p3}(\omega_1) = \hat{\omega}_1^0 = 1; p_1 = p_2 = 1 \tag{21}$$

where $\hat{\omega}_2, \hat{m}_y, \hat{\omega}_1$ are the state variables for the Luenberger observer.

The matrixes are defined as follows:

$$\mathbf{A}_M = \begin{bmatrix} 0 & 333.33 & 0 \\ -1.5 & 0 & 1.5 \\ 18.2 & -2149.8 & -105.7 \end{bmatrix} \tag{22}$$

$$\mathbf{B}_M = \begin{bmatrix} 0 \\ 0 \\ 355.88 \end{bmatrix} \tag{23}$$

$$\mathbf{G} = \begin{bmatrix} 1 & 0 & 0 \\ 0 & 1 & 0 \\ 0 & 0 & 1 \end{bmatrix} \tag{24}$$

$$\mathbf{P} = \begin{bmatrix} 0.0844 & 0.4039 & 0.0058 \\ 0.4039 & 11.1961 & 0.0629 \\ 0.0058 & 0.0629 & 0.0056 \end{bmatrix} \tag{25}$$

where $\Gamma_{qr}^A, \Lambda_{qr}^A, \Gamma_B, \Lambda_B$ are positive coefficients (using a 1×1 matrix): $\Gamma_{qr}^A = \gamma_A = 1, \Lambda_{qr}^A = \lambda_A = 1, \Gamma_B = \gamma_B = 1$ and $\Lambda_B = \lambda_B = 1$.

Following these parameters, our experimental results are shown in Figure 6, including the desired signal graph, the output signal graph of the control object without the controller, the output signal graph of the control object when using the modal controller, and the output signal graph of the control object when using an adaptive controller for the major functions.

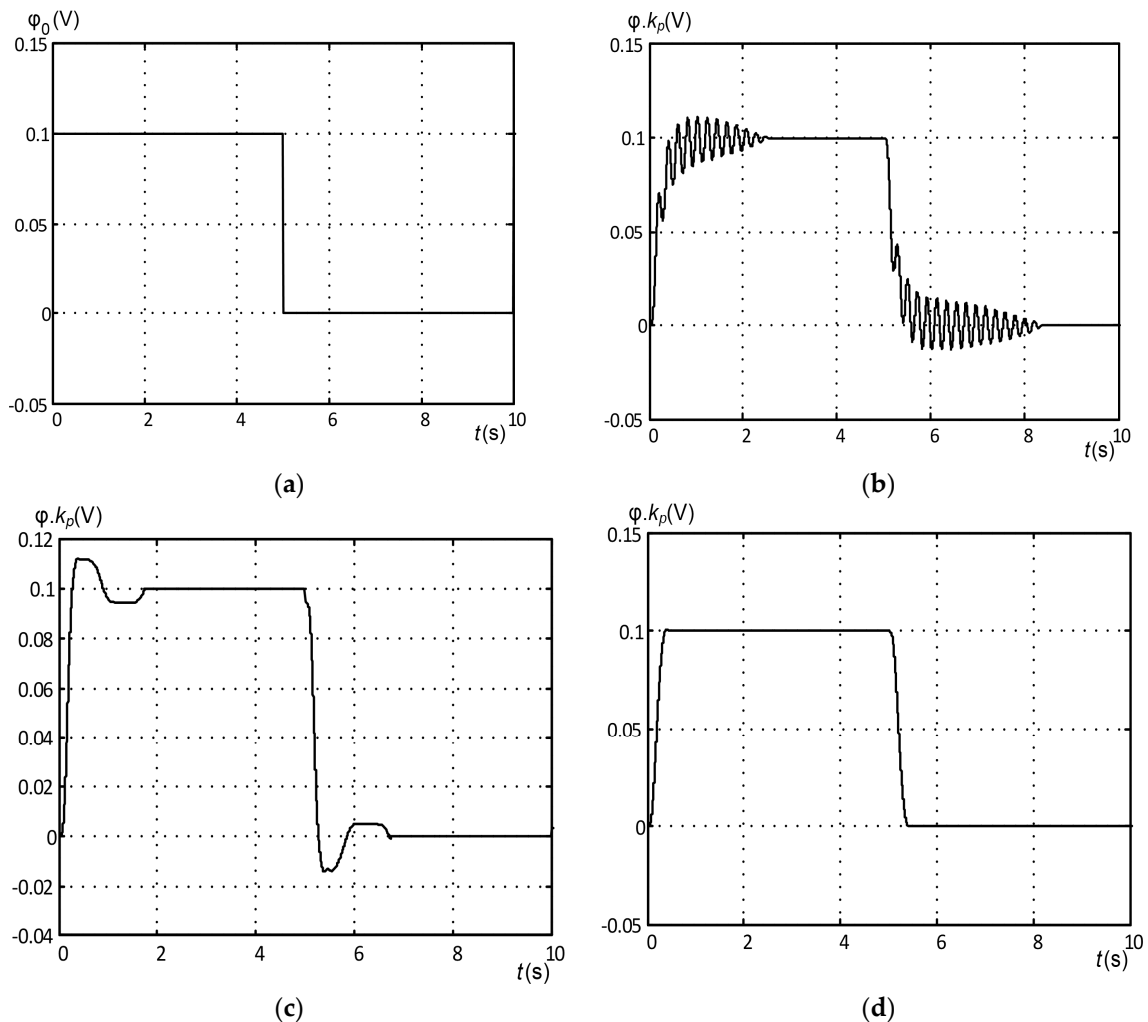


Figure 6. The experimental results: (a) the desired position signal; (b) The output signal of the control object without the controller; (c) the output signal of the control object when using the modal controller; (d) the output signal graph of the control object when using an adaptive controller for the major functions.

Figure 6a shows the desired position signal: a square wave voltage with an amplitude of 0.1 V. It should be noted that the calculation of the angular value must take into account the transmission coefficient of the physical system (0.0412). For example, if the measured voltage value of the rotation angle is 0.1 V, then the actual value of the rotation angle is $\varphi = 0.1/k_p = 0.1/0.0412 = 2.43$ (rad).

Figure 6b, the output signal graph of the control object without the controller, shows the initial control object's elastic oscillations. Figure 6c shows the rotational angle graph of the second disk block when using the modal controller; the elastic vibrations have been extinguished and the rapidity of the system is improved compared to the initial control object. However, the quality of the transition is still poor because there are overshoots and two extremes, and the transition time is still long.

Figure 6d shows the rotational angle graph of the second disk block when using our adaptive controller for the major functions. The elastic vibrations have been extinguished completely,

the rapidity is significantly improved compared to the initial elastic object, and it is close to the rapidity of a hard coupling. The transition process with an adaptive controller is much better than that of the non-adaptive modal controller because we had to approximate some of the parameter values used for building the linearity control object and calculating the modal controller, and in practice, those values may be different from the actual values. In contrast, our adaptive controller can control the object even when some parameter values of the control object are unspecified. Additionally, the control object is nonlinear because of the slit and friction, but these nonlinear elements are also effectively controlled by the adaptive controller. This proposed control system can be applied under different mechanical loads. In such cases, a small error may occur in the position control. However, the goal of vibration reduction is not affected, since the adaptive controller is not influenced by load momentum due to its strong impact on the inner loop (the speed loop).

5. Conclusions

The article has presented a control method based on an adaptive controller for the major functions used to control an object with elastic couplings. The object is nonlinear because of the slit and friction, but the proposed adaptive controller can control the object without knowing the parameter values. The controller's build is optimized so that the movement quality of a drive system with elastic coupling is close to that of one with a hard coupling. The advantage of this proposed method is that the control system can operate well despite unknown object parameter values and with a nonlinear real system. Experimental results confirm the usefulness of our adaptive controller by extinguishing elastic oscillation, reducing transition time, and eliminating overshoot.

Author Contributions: Dung Tran Anh proposed the initial idea. Thang Nguyen Trong and Dung Tran Anh developed the research, analyzed the results, and wrote the article together. Thang Nguyen Trong edited and finalized the article.

Conflicts of Interest: The authors declare no conflict of interest.

References

1. Hori, Y.; Sawada, H.; Chun, Y. Slow resonance ratio control for vibration suppression and disturbance rejection in torsional system. *IEEE Trans. Ind. Electron.* **1999**, *46*, 162–168. [[CrossRef](#)]
2. Preitl, S.; Precup, R.E.; Stinean, A.I.; Dragos, C.A.; Radac, M.B. Control Structures for Variable Inertia Output Coupled Drives. In Proceedings of the 4th IEEE International Symposium on Logistics and Industrial Informatics (LINDI), Smolenice, Slovakia, 5–7 September 2012; pp. 179–184.
3. Amann, N.; Bocker, J.; Prenner, F. Active damping of drive train oscillations for an electrically driven vehicle. *IEEE/ASME Trans. Mechatron.* **2004**, *9*, 697–700. [[CrossRef](#)]
4. Boukhezzar, B.; Siguerdidjane, H. Comparison between linear and nonlinear control strategies for variable speed wind turbines. *Control Eng. Pract.* **2010**, *18*, 1357–1368. [[CrossRef](#)]
5. Salman, S.K.; Teo, A.L. Windmill modeling consideration and factors influencing the stability of a grid-connected wind power-based embedded generator. *IEEE Trans. Power Syst.* **2003**, *18*, 793–802. [[CrossRef](#)]
6. Chang, Y.C.; Yen, H.M. Design of a robust position feedback tracking controller for flexible-joint robots. *IET Control Theory Appl.* **2011**, *5*, 351–363. [[CrossRef](#)]
7. Valenzuela, M.A.; Bentley, J.M.; Lorenz, R.D. Computer-aided controller setting procedure for paper machine drive systems. *IEEE Trans. Ind. Appl.* **2009**, *45*, 638–650. [[CrossRef](#)]
8. Bahr, A.; Beineke, S. Mechanical Resonance Damping in an Industrial Servo Drive. In Proceedings of the 2007 European Conference on Power Electronics and Applications, Aalborg, Denmark, 2–5 September 2007; pp. 1–10.
9. Zhang, G. Speed control of two-inertia system by PI/PID control. *IEEE Trans. Ind. Electron.* **2000**, *47*, 603–609. [[CrossRef](#)]
10. Preitl, S.; Precup, R.E. An extension of tuning relations after symmetrical optimum method for PI and PID controllers. *Automatica* **1999**, *35*, 1731–1736. [[CrossRef](#)]

11. Szabat, K.; Orłowska-Kowalska, T. Performance improvement of industrial drives with mechanical elasticity using nonlinear adaptive Kalman filter. *IEEE Trans. Ind. Electron.* **2008**, *55*, 1075–1084. [[CrossRef](#)]
12. Dhaouadi, R.; Kubo, K.; Tobise, M. Two-degree-of-freedom robust speed controller for high-performance rolling mill drives. *IEEE Trans. Ind. Appl.* **1993**, *29*, 919–926. [[CrossRef](#)]
13. Williams, R.L.; Lawrence, D.A. *Linear State-Space Control Systems*; John Wiley & Sons: Hoboken, NJ, USA, 2007.
14. Jezernik, K.; Sabanovic, A. SMC with disturbance observer for a linear belt drive. *IEEE Trans. Ind. Electron.* **2007**, *54*, 3402–3412.
15. Koronki, P.; Hashimoto, H.; Utkin, V. Direct torsion control of flexible shaft in an observer-based discrete-time sliding mode. *IEEE Trans. Ind. Electron.* **1998**, *45*, 291–296. [[CrossRef](#)]
16. Erenturk, K. Nonlinear two-mass system control with sliding-mode and optimised proportional–integral derivative controller combined with a grey estimator. *IET Control Theory Appl.* **2008**, *2*, 635–642. [[CrossRef](#)]
17. Xu, R.; Özgüner, Ü. Sliding mode control of a class of underactuated systems. *Automatica* **2008**, *44*, 233–241. [[CrossRef](#)]
18. Brock, S.; Łuczak, D.; Nowopolski, K.; Pajchrowski, T.; Zawirski, K. Two Approaches to Speed Control for Multi-Mass System with Variable Mechanical Parameters. *IEEE Trans. Ind. Electron.* **2017**, *64*, 3338–3347. [[CrossRef](#)]
19. Derugo, P.; Szabat, K. Adaptive neuro-fuzzy PID controller for nonlinear drive system. *COMPEL Int. J. Comput. Math. Electr. Electron. Eng.* **2015**, *34*, 792–807. [[CrossRef](#)]
20. Graichen, K.; Zeitz, M. Feedforward control design for finite-time transition problems of nonlinear systems with input and output constraints. *IEEE Trans. Autom. Control* **2008**, *53*, 1273–1278. [[CrossRef](#)]
21. Thomsen, S.; Fuchs, F.W. Flatness Based Speed Control of Drive Systems with Resonant Loads. In Proceedings of the IECON 2010—36th Annual Conference on IEEE Industrial Electronics Society, Glendale, AZ, USA, 7–10 November 2010; pp. 120–125.
22. Tavakoli, M.; Taghirad, H.D.; Abrishamchian, M. Identification and robust H_∞ control of the rotational/translational actuator system. *Int. J. Control Autom. Syst.* **2005**, *3*, 387–396.
23. SerkieS, P. Comparison of the control methods of electrical drives with an elastic coupling allowing to limit the torsional torque amplitude. *EKSPLOATACJA I NIEZAWODNOSC* **2017**, *19*, 203. [[CrossRef](#)]
24. Kang, J.K.; Sul, S.K. Vertical-vibration control of elevator using estimated car acceleration feedback compensation. *IEEE Trans. Ind. Electron.* **2000**, *47*, 91–99. [[CrossRef](#)]
25. Katsura, S.; Ohnishi, K. Absolute stabilization of multimass resonant system by phase-lead compensator based on disturbance observer. *IEEE Trans. Ind. Electron.* **2007**, *54*, 3389–3396. [[CrossRef](#)]
26. Katsura, S.; Matsumoto, Y.; Ohnishi, K. Modeling of force sensing and validation of disturbance observer for force control. *IEEE Trans. Ind. Electron.* **2007**, *54*, 530–538. [[CrossRef](#)]
27. De Araujo, P.B.; Zanetta, L.C. Pole placement method using the system matrix transfer function and sparsity. *Int. J. Electr. Power Energy Syst.* **2001**, *23*, 173–178. [[CrossRef](#)]
28. Peeters, B.; De Roeck, G. Stochastic system identification for operational modal analysis: A review. *J. Dyn. Syst. Meas. Control* **2001**, *123*, 659–667. [[CrossRef](#)]
29. Duan, G.R.; Patton, R.J. Robust fault detection using Luenberger-type unknown input observers—a parametric approach. *Int. J. Syst. Sci.* **2001**, *32*, 533–540. [[CrossRef](#)]
30. Hu, X.; Sun, F.; Zou, Y. Estimation of state of charge of a lithium-ion battery pack for electric vehicles using an adaptive Luenberger observer. *Energies* **2010**, *3*, 1586–1603. [[CrossRef](#)]

